

# Supporting Information

Khan et al. 10.1073/pnas.1412227111

## SI Materials and Methods

**Electrochemical Experiments.** Electrochemical measurements (i.e., cyclic voltammetry and electrochemical impedance spectroscopy) were made using a Bio-Logic SP-200 potentiostat. A saturated Ag–AgCl reference electrode and a platinum mesh counter-electrode were used in all of the experiments, with copper acting as the connection to the eutectic gallium indium (EGaIn; purchase from Indium Corporation and 5N) working electrode. Copper was chosen because it makes excellent electrical contact with EGaIn. X-ray photoelectron spectroscopy measurements detected no copper at the interface of EGaIn–electrolyte after exposing the EGaIn to the copper wire. Care was taken to minimize or eliminate the exposure of the copper electrode to the solution. In experiments in which the copper was exposed, there was no measurable effect on the interfacial tension at each potential. Unless otherwise stated, all experiments took place in 1 M NaOH.

**Area Measurements.** EGaIn drops of  $\sim 30$   $\mu\text{L}$  were placed in a plastic Petri dish filled with 1 M NaOH. A copper wire was connected to the top of the drop, and a video camera was placed underneath the transparent Petri dish. Oxidative potentials were applied from  $-1.4$  to  $-0.5$  V vs. the reference electrode (placed  $\sim 5$  cm away from the liquid metal), in 100-mV increments. A camera filmed the drop for 2 min after each incremental change in voltage, or until it separated from the copper wire due to excessive spreading. The images were then analyzed in ImageJ to determine the areal footprint, as illustrated in Fig. S1.

**Interfacial Tension Measurements.** The interfacial tension was determined as a function of potential by using the potentiostat in conjunction with a goniometer (First Ten Angstroms 1000B). Sessile droplets of EGaIn, ranging in volume from 25 to 50  $\mu\text{L}$ , were placed on the tip of a small, exposed copper wire (Fig. S2). The goniometer determined the volume and the interfacial tension and surface area as a function of voltage. The potential was increased in increments of 100 mV from  $-2$  to  $-0.8$  V vs. the reference electrode. At potentials more negative than  $-2$  V, bubbles formed rapidly on the surface of the EGaIn from reductive electrolysis of water. At potentials more positive than  $-0.7$  V, the shape of the EGaIn drop flattened to such an extent that interfacial tension could no longer be estimated using the goniometer, although the metal did continue to spread until it disconnected from the electrode.

**Capacitance Measurements.** The capacitance was measured by electrochemical impedance spectroscopy (EIS). An EIS scan was performed at each potential used in the interfacial tension measurements, from 200 kHz to 1 Hz. Fitting software determined the double-layer capacitance from the resulting Nyquist plots (examples of which can be seen in Fig. S3). This fitting was accomplished by assuming a solution resistance in series with an interfacial resistance and a constant phase element in parallel. For the region where no oxide was present (shaded region of Fig. 1C), the interfacial resistance was necessary to adequately fit the low-frequency end of the spectrum (down to 1 Hz). However, the high-frequency region ( $10^2$ – $10^4$  Hz)—where double-layer capacitance dominates the response—could be fit satisfactorily with a simple solution resistance and constant phase element in series with minor change in the capacitance values. For the potential region where the oxide layer was present, the model was fit only to the high-frequency

capacitive region, whereas the low-frequency end that reflects more complicated chemistry, e.g., adsorption of hydroxyl ions (1, 2), was not analyzed in the present work. The specific capacitance was determined by dividing the capacitance by the surface area determined by the goniometer at each potential. Although we assumed pseudo-steady-state growth of the oxide layer, we ascertained similar Nyquist plots and capacitance values to those given by Macdonald et al. (1) for Al (a metal from the same column of the periodic table that also forms a passivating oxide) over the entire range of potentials.

The capacitive energy ( $U$ ) was calculated by first estimating the potential ( $E$ ) relative to the potential of zero charge ( $E_{PZC}$ ), determined from Fig. 1C, and using the equation  $U = 1/2 C(E - E_{PZC})^2$ . The capacitance values obtained from a best fit of the shaded region of Fig. 1C—approximately  $C = 27$   $\mu\text{F}/\text{cm}^2$ —agreed with the values measured directly via impedance spectroscopy at reducing potentials (Fig. 1E).

**Reversibility Measurements.** We measured the interfacial tension of the metal after stepping the voltage up and down several times. These reversibility measurements were performed by multistep chronoamperometry in the same setup described previously to measure interfacial tension (i.e., sessile drop). In this case, the potential was varied between  $-1.5$ ,  $-1.25$ , and  $-1.0$  V vs. Ag/AgCl, and held at each potential for 5 s while measuring continuously the interfacial tension of a sessile drop.

**Capillary Length.** To estimate the interfacial tension beyond the measuring capability of our instruments (i.e., at voltages greater than or equal to the critical voltage of  $-0.6$  V, at which point the metal spreads dramatically), a scaling analysis based on the capillary length of the drop was used. The capillary length is based on a ratio between gravitational and interfacial forces, as shown in Eq. S1,

$$L = \sqrt{\frac{\gamma}{\rho g}}, \quad [\text{S1}]$$

where  $L$  is the characteristic capillary length,  $\rho$  is the density of the EGaIn, and  $g$  is the acceleration due to gravity. We used the ratio of capillary lengths to estimate the interfacial tension relative to a known value, as shown in Eq. S2,

$$\frac{L_2}{L_1} = \frac{\sqrt{\frac{\gamma_2}{\rho g}}}{\sqrt{\frac{\gamma_1}{\rho g}}}, \quad [\text{S2}]$$

where the subscripts 2 and 1 represent droplets at two different potentials. Algebraic rearrangement yields Eq. S3,

$$\gamma_2 = \gamma_1 \left( \frac{L_2}{L_1} \right)^2. \quad [\text{S3}]$$

When the drop is roughly spherical yet coated with oxide (at  $-1.3$  V),  $\gamma_1 = 330$  mN/m and the characteristic length is the radius ( $L_1 = 2$  mm). When the droplet spreads dramatically (greater than  $-0.6$  V), the capillary length is half the thickness (estimated to be  $L_2 = 0.15$  mm based on a  $>10\times$  increase in areal footprint, according to Fig. 1). Using this scaling,  $\gamma_2 \sim 2$  mN/m.

Repeating this analysis, but using the last measurable tension ( $-0.7$  V),  $\gamma_1 = 49$  mN/m and the characteristic length is half the height ( $L_1 = 0.8$  mm). Using this scaling,  $\gamma_2 \sim 2$  mN/m.

**EGaIn Spreading (Movies S1–S4).** For **Movie S1**, a drop of EGaIn was dispensed from a stainless steel syringe needle and placed onto a glass slide in 1 M NaOH. The syringe needle acted as the electrical connection to the EGaIn, while a counterelectrode and reference electrode were placed in the solution. The applied voltage (relative to the open-circuit potential,  $-1.5$  V vs. Ag–AgCl) was increased from 0 to 1 V. Video was taken with the goniometer. Analyzing the behavior of the metal in this configuration has two challenges: (i) The droplets often detach from the syringe needle during spreading, and (ii) it is possible for small amounts of metal to flow from the syringe into the spreading droplet. Despite these complications, we report this configuration to illustrate the thread of liquid metal that often forms to maintain the connection between the syringe and the spreading droplet. This configuration also proves that the copper wire (as shown in Fig. S2) does not interfere with the spreading.

For **Movie S2**, similar conditions were used, with the video being taken by a digital overhead camera while connecting the EGaIn to the working electrode by an insulated copper wire that penetrates through the substrate to contact the droplet on the bottom side (Fig. S2). In this configuration, volume is conserved and the electrical connectivity is only lost when the spreading EGaIn droplet starts forming finger instabilities. The analysis in Fig. 2 was completed using measurements with this configuration.

For **Movie S3**, a droplet of EGaIn was placed on the apparatus shown in Fig. S2, immersed in 1 M NaOH. A potential of 0.5 V was applied to the droplet, and the droplet spread out to a thermodynamic equilibrium. A pipette was then pushed into the drop and dragged out. This changed temporarily the shape of the drop; however, after only a few seconds, the drop returned to its equilibrium state. When the potential was removed, the droplet once again became spherical due to removal of the oxide.

**Movie S4** shows a 1-V potential applied to an EGaIn drop in 1 M NaF. In this case, the spreading begins to occur, but is ultimately limited by the growth of the oxide layer on the surface. The formation of a thicker oxide is visually apparent and arrests further spreading.

**Liquid Metal Flowing into a Capillary (Movie S5).** A drop of liquid metal—the “reservoir”—was brought in contact with a 70-mm-long borosilicate glass capillary ( $0.9$  mm  $\pm$   $0.1$  mm i.d.) prefilled with 1 M NaOH. To achieve a spherical drop shape, a small amount ( $\sim 0.25$  mL) of electrolyte (1 M NaOH) was used around the edge of the drop, but otherwise it rested on a plastic Petri dish in an air atmosphere. Application of an oxidative bias to the metal relative to an electrode contacting the electrolyte at the other end of the capillary causes the metal to flow into the capillary despite the smaller radius of curvature of the leading interface, which suggests the leading interface has a lowered interfacial tension. The capillary was oriented at an angle of  $10$ – $20^\circ$  relative to the plane of the substrate such that the metal moves uphill against gravity.

**Directional EGaIn Flow (Movie S6).** An EGaIn drop was placed on top of a T-shaped recess composed of a sheet of acrylic patterned with a laser cutter (Universal VLS3.50). The acrylic piece was placed on a Petri dish filled with 1 M NaOH solution. A copper wire was then inserted into the EGaIn drop and 5-V DC potential was applied with a Keithley 3390 function generator. Although lower voltages are sufficient to allow directional control with a three-electrode system, a two-electrode system was used for simplicity. A copper counterelectrode was then placed in the solution at various points along the channel and the EGaIn flowed preferentially toward the counterelectrode.

**EGaIn Fibers (Movie S7).** EGaIn was extruded out of Tygon plastic tubing with an i.d. of 0.5 mm at a rate of 20 mL/h, using a Chemxy Fusion 100 syringe pump, into a plastic cuvette filled with 1 M NaOH. A working electrode was attached to the syringe needle (to provide electrical contact with the EGaIn) and a copper counterelectrode was placed in the cuvette. A 5-V DC potential was applied with a Keithley 3390 function generator. In the absence of applied potential, droplets form as the metal emerges from the end of the tubing. When the droplets reach a critical size, they fall due to gravity, as expected. In the presence of applied oxidative potential, fibers form due to the presence of the oxide skin and presumably due to the lowering of the interfacial tension.

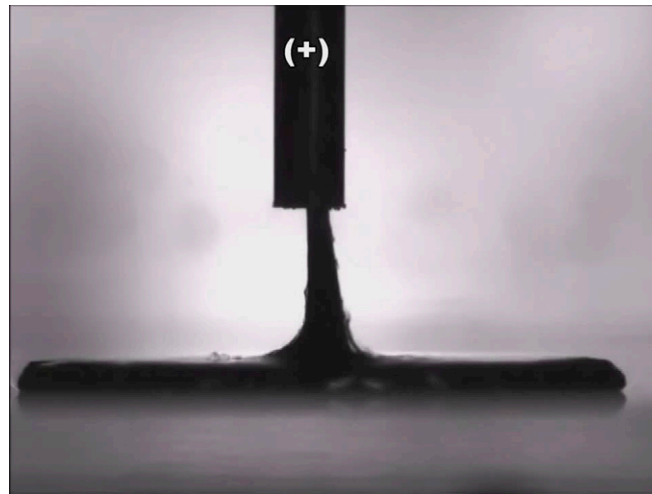
**Asymmetric Dewetting (Movie S8).** A sessile drop of liquid metal was spread on a dry plastic Petri dish. The presence of an oxide layer on the metal causes it to adhere to the substrate. It also allows the droplet to be physically spread on the surface to assume a low contact angle, which illustrates the hysteretic nature of the contact angle of the oxide-coated metal on dry surfaces. The droplet was then submerged in deionized water. A 100- $\mu$ m-diameter tungsten wire touched the top surface of the drop (cathode) and another piece of tungsten wire—the anode—was placed  $\sim 5$  mm away from the right edge of the drop. A potentiostat applied 5 V initially for  $\sim 2$  s, 0 V for  $\sim 2$  s, and 5 V for  $\sim 1$  s. At 0 V, the metal stops moving because the oxide reforms conformally on the droplet. The goniometer measured the contact angle on both sides of the drop versus time. The contact angle changes most dramatically on the right side because the oxide is being removed preferentially there by electrochemical reduction. Although the contact angle is asymmetric, it also increases on the left side due to conservation of mass and the droplet pinning to the substrate.

**Recapillarity-Induced Actuation in Microchannels (Movie S9).** T-shaped microfluidic channels composed of polydimethylsiloxane (SYLGARD-184 from Dow) were fabricated via replica molding. A syringe was used to inject liquid metal into this T-shaped channel in the absence of electrolyte. Electrolyte was then added to the outlet reservoir. These experiments used 1 M NaF solution as the electrolyte and either copper or tungsten wire as the electrodes. As soon as the reducing potential was applied, the metal underwent capillary action (recapillarity) in the absence of the oxide skin. When the potential was turned off, the metal stopped moving immediately, presumably due to the reformation of the oxide layer.

1. Macdonald DD, Real S, Smedley SI, Urquidí-Macdonald M (1988) Evaluation of alloy anodes for aluminum-air batteries. IV. Electrochemical impedance analysis of pure aluminum in at 25°C. *J Electrochem Soc* 135:2410–2414.

2. deWit JHW, Lenderink HJW (1996) Electrochemical impedance spectroscopy as a tool to obtain mechanistic information on the passive behaviour of aluminium. *Electrochim Acta* 41:1111–1119.





**Movie S1.** Application of an oxidative bias to a droplet of the liquid metal lowers the interfacial tension and allows the drop to spread due to gravitational forces.

[Movie S1](#)



**Movie S2.** A top-down view of the spreading shown in [Movie S1](#). Here, an electrode protrudes from the substrate to contact the liquid metal.

[Movie S2](#)



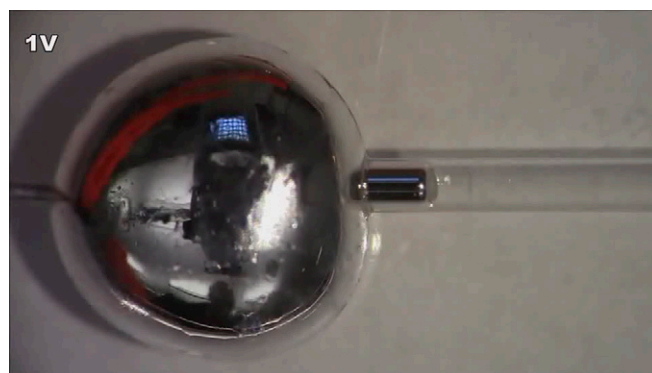
**Movie S3.** After mechanically distorting a droplet of the metal, it returns to an equilibrium shape.

[Movie S3](#)



**Movie S4.** In pH-neutral electrolytes, the metal spreads partially before it glazes over with a thicker oxide layer.

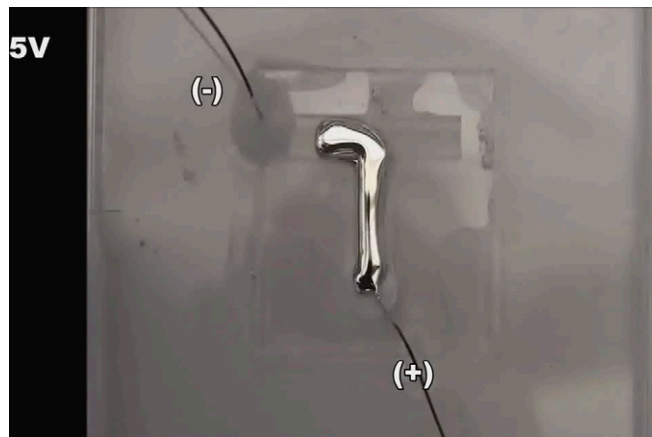
[Movie S4](#)



**Movie S5.** The liquid metal flows uphill into a glass capillary upon application of an oxidative bias to the spherical reservoir of metal located at the tip of the capillary. The perspective is top-down.

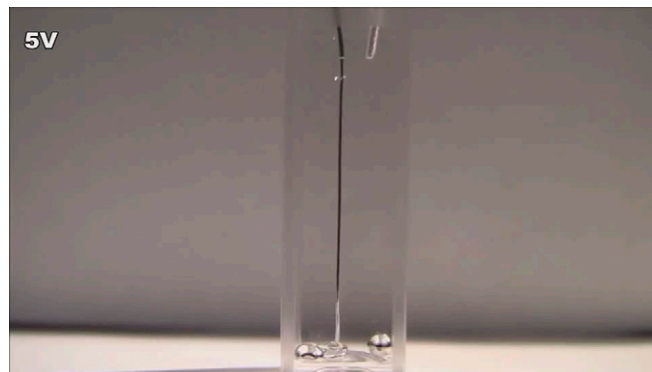
[Movie S5](#)





**Movie S6.** The metal spreads and can change shape in an open channel in response to an oxidative potential. It is apparent that hydrogen bubbles form at the counter electrode.

[Movie S6](#)



**Movie S7.** A syringe pump forces metal out of a plastic tube and into an electrolyte solution. In the absence of potential, droplets of metal periodically fall from the end of the tubing. Application of an oxidative bias to the liquid metal causes it to form fibers.

[Movie S7](#)

